

Modeling of an Interior Permanent Magnet Synchronous Motor with Two Independent Stator Windings using Rotor Reference Frame

Onah. C. O.¹, Obe. E. S.², Agber. J. U.³

¹Lecturer, Department of Electrical and Electronics Engineering, University of Agriculture, Makurdi, Nigeria

²Professor, Department of Electrical and Electronics Engineering, University of Nigeria, Nsukka

³Professor, Department of Electrical and Electronics Engineering, University of Agriculture, Makurdi, Nigeria

Abstract: Dynamic modeling of permanent magnet synchronous machines has preoccupied electrical machines analysis for a long time, as evidenced by the existence of various types of models. This paper presents a dynamic model of an interior permanent magnet synchronous motor (IPMSM) with two independent stator windings using rotor reference frame. The comprehensive mathematical model using Park's transformation equation to define the performance characteristics of the proposed motor winding configuration is presented. A d-q equivalent circuit of the motor suitable for dynamic analysis is deduced from the mathematical model in machine variables. Simulation of the dynamic model of the motor winding configuration is performed on a 2.98 kW, 4-pole, 415 V, 50 Hz IPMSM in MATLAB/Simulink environment and results presented.

Keywords: D-q equivalent circuit, Dynamic modeling, IPMSM, Rotor reference frame, Stator windings

Date of Submission: 21-01-2020

Date of Acceptance: 12-02-2020

I. Introduction

The concept of dual stator winding machine applications can be found in some papers published as early as the beginning of 20th century [1]. However, high performance control of these machines was difficult due to the absence of power electronic converters and the incomplete analysis of the machines due to the immaturity of machine theory, numerical simulation and analytical methodologies. Recently, dual winding machines of various types are being considered for various motoring and generating applications, since two sets of stator windings offer the possibility of more flexible energy conversion and control [2]. For example, energy can be transferred not only between stator and rotor like what is obtainable in single winding machines, but also indirectly between the two sets of stator windings.

Generally, in terms of the stator winding, dual winding machines are categorized as split-wound and self-cascaded machines [3]. The split-wound dual winding machine was introduced in 1930's as means of increasing the total power capability of large synchronous generators. Since then, this concept has been utilized in many other applications ranging from synchronous machines with AC and DC outputs as part of uninterrupted power supplies [4]. The split-wound synchronous machine with either round or salient-pole rotor structure has two sets of similar but separate three-phase windings wound for the same number of poles. The squirrel-cage machine version also has two symmetric but separate three-phase stator winding sets having the same pole number. Since the two sets of windings have the same pole number, they are coupled together resulting in significant circulating currents in the presence of unavoidable unbalances in the supply voltages [5]. The second type of dual winding machines, which is referred to as the "self-cascaded machine" has two sets of stator windings with different pole numbers but the same number of phases and sharing the same stator core. This requires a special rotor structure that has nested loops to incorporate the effects of cascade connection [5, 6]. Due to the difference in rotor structures, the brushless doubly-fed machine can be further categorized into brushless doubly-fed induction machines and brushless doubly-fed synchronous reluctance machines. The special rotor structure increases the cost of the machine, the efficiency is relatively low, but has potential utility in drive applications with a narrow speed range.

The steady state performance analysis of a connection scheme that improved the power factor and torque with a lower magnetizing current for a line-start synchronous reluctance motor was presented elsewhere [7]. The paper reported the machine stator winding, which was split into two equal halves with one connected to the mains and the other connected to a balanced capacitor. There was an improved performance of the machine when the capacitor value was such that the winding to which it was connected, operated at or very close to resonance in the d-axis. Currents in both windings contributed positively to torque production and external control circuitry was not required. Steady-state equations derived from the d-q model gave a direct insight on the operating limits and how the capacitance aided the machine torque and power factor by boosting its direct

axis reactance. However, the quadrature axis reactance remained fairly constant. An equivalent circuit was also deduced from the steady state equations, from which an explicit expression for input impedance of the new machine can be derived. The paper further examined the conditions for unity-power factor at varying load conditions. A comparison with conventional single-winding synchronous reluctance motor was given. Finally, the author concluded that such comparison was fair because both machines had equal amount of copper and iron.

Experimental results were provided to validate the analytical results. In this paper, the winding adopted is similar to the one utilized in the paper [7] but applied to interior permanent magnet synchronous motor.

II. Material and Methods

2.1 Machine Description

The proposed interior permanent magnet synchronous motor is modeled as a dual stator winding interior permanent magnet synchronous motor having two independent stator windings. The two independent stator windings are magnetically coupled through the stator core but electrically isolated. For the purposes of distinction, one of the two sets of three-phase stator windings is referred to as the main winding and is connected to the three-phase mains supply. The main winding is designated as ABC. The second set of the stator windings is referred to as the auxiliary winding, represented as abc and connected to a balanced set of capacitors for leading current injection. The injection of leading current will enhance the electromagnetic torque of the machine. The machine winding configuration as adopted in this paper is as depicted in Figure 1.

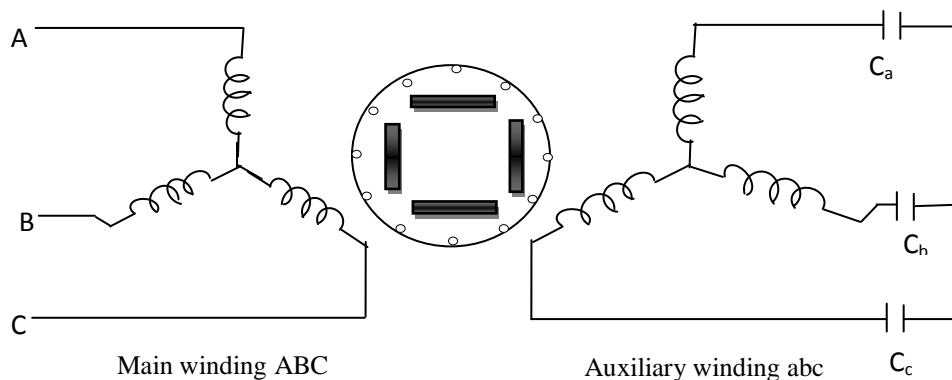


Figure 1: Machine Winding arrangement of Main and Auxiliary Windings

2.2 Model of the Machine

In order to develop the mathematical model that defines the characteristics of the type of motor winding configuration adopted in this paper, certain simplifying assumptions and approximations are made, which include:

- i) The set of three-phase stator winding is symmetrical.
- ii) The two sets of stator windings ABC and abc are magnetically coupled through the stator core but electrically isolated.
- iii) The two sets of stator windings are identical and wound for the same number of poles.
- iv) There is no displacement between the two sets of stator windings.
- v) Saturation effects are neglected.

The performance characteristics of the proposed IPMSM structure based on the simplified assumptions and approximations can be described by the electrical voltage equations expressed in machine variables as presented in equations (1) - (3).

$$V_{ABCs} = r_{ABCs} i_{ABCs} + p \lambda_{ABCs} \quad (1)$$

$$0 = r_{abcs} i_{abcs} + p \lambda_{abcs} + V_{Cabcs} \quad (2)$$

$$0 = r_{qdr} i_{qdr} + p \lambda_{qdr} \quad (3)$$

where,

$$\left. \begin{aligned} V_{ABCs} &= [V_{As} \quad V_{Bs} \quad V_{Cs}]^t \\ i_{ABCs} &= [i_{As} \quad i_{Bs} \quad i_{Cs}]^t \\ \lambda_{ABCs} &= [\lambda_{As} \quad \lambda_{Bs} \quad \lambda_{Cs}]^t \end{aligned} \right\} (4)$$

$$\left. \begin{aligned} i_{qdr} &= [i_{qr} \quad i_{dr}]^t \\ \lambda_{qdr} &= [\lambda_{qr} \quad \lambda_{dr}]^t \end{aligned} \right\} \quad (5)$$

$$\left. \begin{aligned} V_{CabcS} &= [V_{Cas} \quad V_{Cbs} \quad V_{Ccs}]^t \\ i_{abcS} &= [i_{as} \quad i_{bs} \quad i_{cs}]^t \\ \lambda_{abcS} &= [\lambda_{as} \quad \lambda_{bs} \quad \lambda_{cs}]^t \end{aligned} \right\} \quad (6)$$

Subscripts *s* and *r* in equations (1) - (6) represent variables related to the stator and rotor windings, while ABC and abc signify the main and auxiliary windings respectively.

The flux linkage equations are also expressed by equations (7) - (9).

$$\lambda_{ABCs} = L_{ABCs} i_{ABCs} + L_{ABC-abc} i_{abcS} + L_{ABC-qdr} i_{qdr} + \lambda_{mA} \quad (7)$$

$$\lambda_{abcS} = L_{abc-ABC} i_{ABCs} + L_{abcS} i_{abcS} + L_{abc-qdr} i_{qdr} + \lambda_{ma} \quad (8)$$

$$\lambda_{qdr} = L_{qdr-ABC} i_{ABCs} + L_{qdr-abc} i_{abcS} + L_{qdr} i_{qdr} + \lambda_{mqdr} \quad (9)$$

2.3 Voltage Equations of the Proposed Motor in Rotor Reference Frame

In order to eliminate the sinusoidal coupling in the modeled equations in machine variables, the stator and rotor equations are referred to a common reference. In this paper, the general equations are referred to the rotor reference frame, since time varying inductances of the synchronous machine are said to be eliminated once the inductances are fixed on the rotor [8, 9, 10]. From equations (4) and (6) - (8), which defined the stator variables and taking θ_r as the angular position of the rotor reference frame, the change of variable, which allows a transformation of the stator phase variables to rotor reference frame is in equation (10).

$$K_{qdos} = T(\theta_r) K_{ABCs} \quad (10)$$

while the inverse is given by equation (11).

$$K_{ABCs} = [T(\theta_r)]^{-1} K_{qdos} \quad (11)$$

where

$$K_{qdos} = [K_{qs} \quad K_{ds} \quad K_{os}]^t \quad (12)$$

and K can be current, voltage or flux linkage.

The transformation matrix $T_{dq0}(\theta_r)$ is given in equation (13) and the inverse defined by equation (14) [8, 11, 12].

$$T_{dq0}(\theta_r) = \frac{2}{3} \begin{bmatrix} \cos\theta_r & \cos\left(\theta_r - \frac{2\pi}{3}\right) & \cos\left(\theta_r + \frac{2\pi}{3}\right) \\ \sin\theta_r & \sin\left(\theta_r - \frac{2\pi}{3}\right) & \sin\left(\theta_r + \frac{2\pi}{3}\right) \\ \frac{1}{2} & \frac{1}{2} & \frac{1}{2} \end{bmatrix} \quad (13)$$

$$[T_{dq0}(\theta_r)]^{-1} = \begin{bmatrix} \cos\theta_r & \sin\theta_r & 1 \\ \cos\left(\theta_r - \frac{2\pi}{3}\right) & \sin\left(\theta_r - \frac{2\pi}{3}\right) & 1 \\ \cos\left(\theta_r + \frac{2\pi}{3}\right) & \sin\left(\theta_r + \frac{2\pi}{3}\right) & 1 \end{bmatrix} \quad (14)$$

When equations (10), (11) and (13) are applied in equations (1) – (3), the stator voltage equations in rotor reference frame are given by equations (15) and (16), while the rotor voltage equations are given in equation (17).

$$\left. \begin{aligned} V_{q1} &= r_1 i_{q1} + p\lambda_{q1} + \omega_r \lambda_{d1} \\ V_{d1} &= r_1 i_{d1} + p\lambda_{d1} - \omega_r \lambda_{q1} \\ 0 &= r_2 i'_{q2} + p\lambda'_{q2} + \omega_r \lambda'_{d2} + V_{Cq2} \\ 0 &= r_2 i'_{d2} + p\lambda'_{d2} - \omega_r \lambda'_{q2} + V_{Cd2} \end{aligned} \right\} \quad (16)$$

Rotor voltage equations:

$$\left. \begin{aligned} 0 &= r_{qr} i'_{qr} + p\lambda'_{qr} \\ 0 &= r_{dr} i'_{dr} + p\lambda'_{dr} \end{aligned} \right\} \quad (17)$$

The corresponding flux linkage equations in rotor reference frame are given also by equations (18) - (20).

$$\left. \begin{aligned} \lambda_{q1} &= L_{l1} i_{q1} + L_{mq} (i_{q1} + i'_{q2} + i_{qr}) \\ \lambda_{d1} &= L_{l1} i_{d1} + L_{md} (i_{d1} + i'_{d2} + i'_{dr}) + \lambda'_m \\ \lambda'_{q2} &= L_{l2} i'_{q2} + L_{mq} (i_{q1} + i'_{q2} + i_{qr}) \\ \lambda'_{d2} &= L_{l2} i'_{d2} + L_{md} (i_{d1} + i'_{d2} + i'_{dr}) + \lambda'_m \end{aligned} \right\} \quad (18)$$

$$\left. \begin{aligned} \lambda'_{qr} &= L_{lqr} i'_{qr} + L_{mq} (i_{q1} + i'_{q2} + i_{qr}) \\ \lambda'_{dr} &= L_{ldr} i'_{dr} + L_{md} (i_{d1} + i'_{d2} + i'_{dr}) + \lambda'_m \end{aligned} \right\} \quad (20)$$

The voltage equations of auxiliary winding are different from the main winding because no voltage is applied directly to the winding. Capacitors are rather connected to the auxiliary winding as in Figure 1. Thus, it is important to state the equations for a capacitor in the rotor reference frame as described in equation (21) [7].

$$\left. \begin{aligned} pV_{Cd2} &= \frac{i'_{d2}}{C} + \omega_r V_{Cq2} \\ pV_{Cq2} &= \frac{i'_{q2}}{C} - \omega_r V_{Cd2} \end{aligned} \right\} \quad (21)$$

where,

V_{Cd2} and V_{Cq2} are the capacitor direct and quadrature axes voltages respectively while ω_r is the synchronous angular frequency in radians per second and C is the capacitance per phase.

2.4 The Electromagnetic Torque Equation

The electromagnetic torque of the proposed machine is obtained from the sum of the input power supplied to all the windings including the rotor cage as given in equation (22). The electromagnetic torque equation shows that both windings contribute positively to the torque production.

$$T_e = \frac{3}{2} \frac{P}{2} \left[(L_{d1} - L_{q1}) i_{q1} i_{d1} + (L_{d2} - L_{q2}) i'_{q2} i'_{d2} + (L_{md} - L_{mq}) (i_{d2} i_{q1} + i'_{q2} i_{d1}) + (L_{md} i'_{dr} i_{q1} - L_{mq} i'_{qr} i_{d1}) + (L_{md} i'_{dr} i'_{q2} - L_{mq} i'_{qr} i'_{d2}) + \lambda'_m (i_{q1} + i'_{q2}) \right] \quad (22)$$

Since the proposed motor is an electromechanical device, there is need for an equation to describe the coupling nature of the electrical and mechanical systems which is given by equation (23).

$$T_e = J \left(\frac{2}{P} \right) p\omega_r + T_L \quad (23)$$

The derivative of the speed equation is expressed in equation (24).

$$p\omega_r = \frac{(T_e - T_L) P}{2J} \quad (24)$$

where,

J is moment of inertia, T_L is the load torque and ω_r is the angular velocity of the rotor.

2.4 D-q Equivalent Circuit of the Motor

The equivalent circuit of the model configuration adopted can be developed by neglecting the mutual leakage inductance between the winding sets ABC and abc. Thus, the equations used for the development of d-q equivalent circuit of the proposed IPMSM with rotor cage are summarized in equations (15) - (20) while the q-axis and d-axis equivalent circuits are presented in Figures 2 and 3 respectively

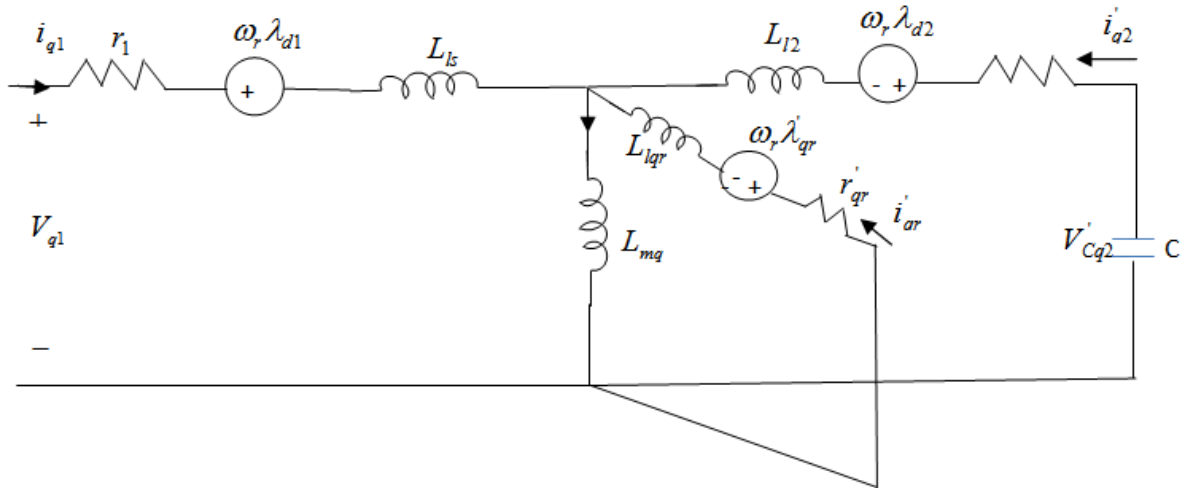


Figure 2: Q-axis Equivalent Circuit of an IPMSM with two independent stator windings, Rotor Cage and Capacitance Injection

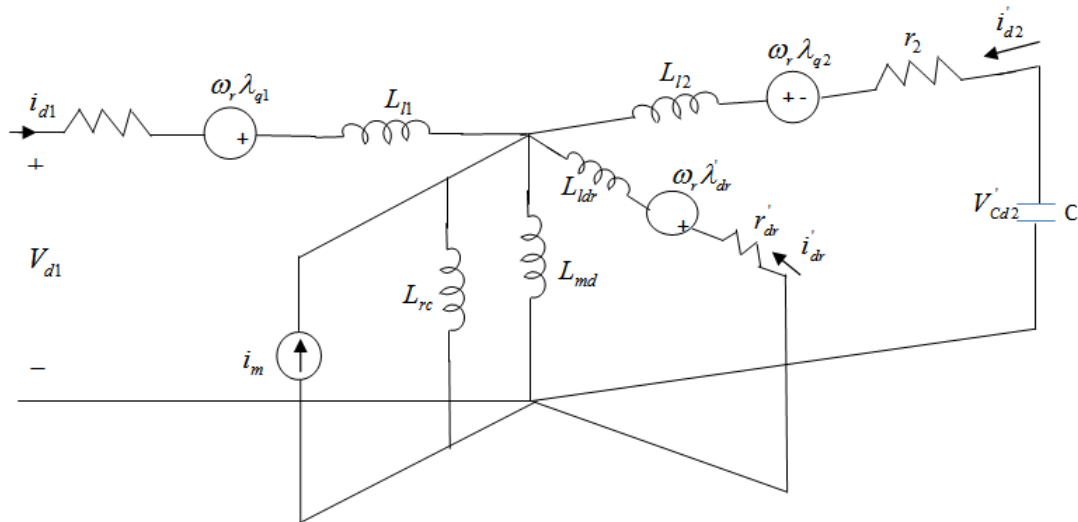


Figure 3: D-axis Equivalent Circuit of an IPMSM with two independent stator windings, Rotor Cage and Capacitance Injection

III. Result

This section presents the dynamic performance of the proposed machine with the aid of computer model simulated in MATLAB/Simulink environment. The model is simulated using the derived mathematical equations of the line-start interior permanent magnet synchronous motor with two independent stator windings as provided in equations (15) - (24). Figure 4 shows the complete Simulink block diagram of the proposed model. The simulation was set to run for 10 s with the load torque applied at 5 s. Parameters of the 2.98 kW interior permanent magnet synchronous motor are shown in Table 1.

Table 1: Machine Parameters

Frequency, $f = 50$ Hz No. of Poles, $P = 4$

Stator leakage Inductance, $L_{ls} = 0.0028$ H q-axis Inductance, $L_{mq} = 0.0441$ H

Moment of inertia, $J = 0.42$ Kg m^2 d-axis Inductance, $L_{md} = 0.0206$ H

q-axis Cage Inductance, $L'_{lkq} = 0.0057$ H d-axis Cage Inductance, $L'_{lkd} = 0.0057$ H

Stator Resistance, $r_s = 0.301$ Ω

q-axis Cage Rotor Resistance, $r'_{kq} = 1.912$ Ω

d-axis Cage Rotor Resistance, $r'_{kd} = 0.957$ Ω Permanent magnet Flux linkage, $\lambda_m = 0.8$ Wb turn

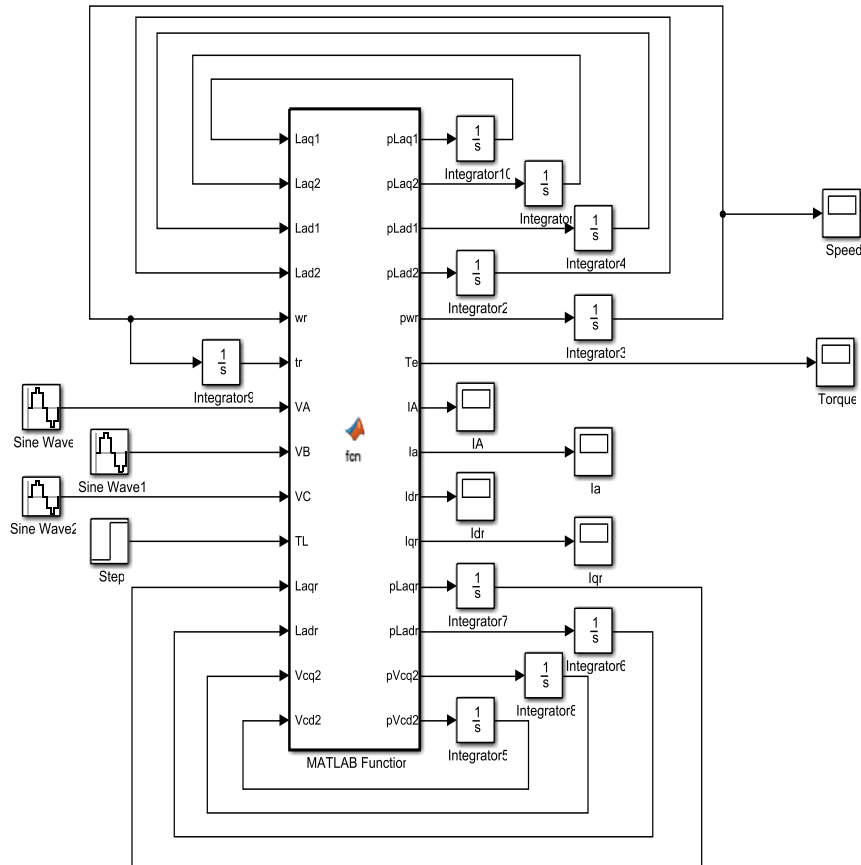


Figure 4: Simulink Block Diagram for Dynamic Simulation of the Proposed Motor

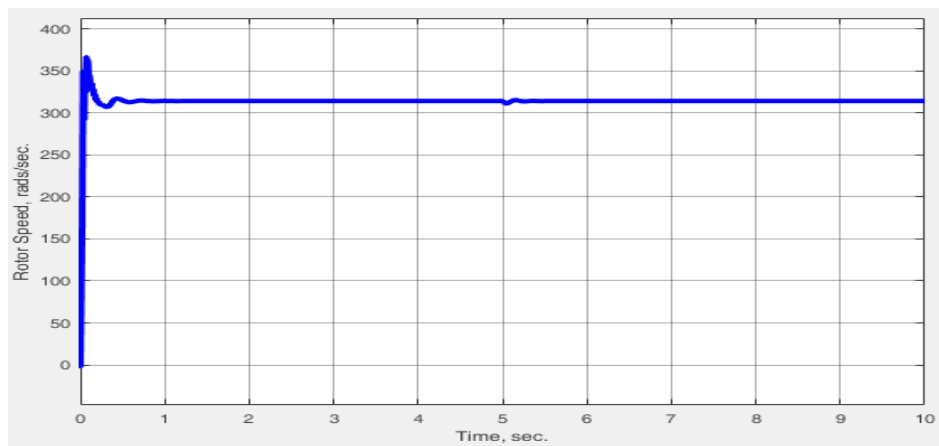


Figure 5: Rotor Speed Response of the Proposed Machine

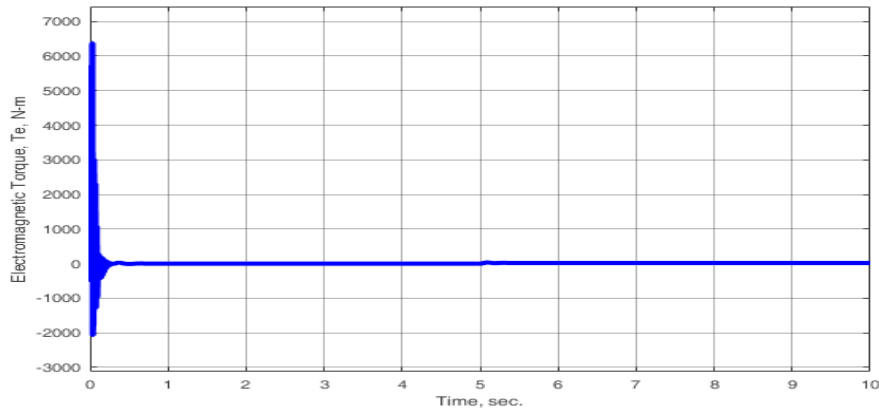


Figure 6: Electromagnetic Torque of the Proposed Machine

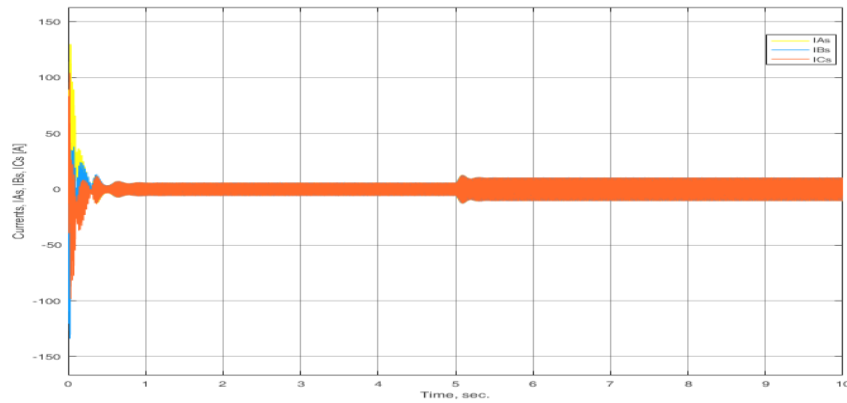


Figure 7: Main Winding Currents of the Proposed Machine

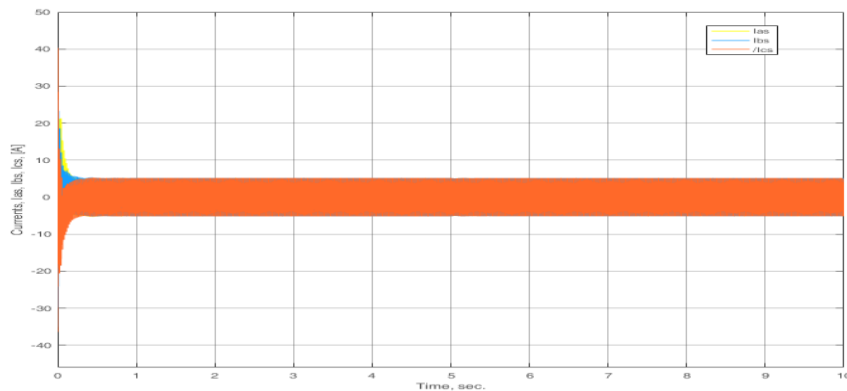


Figure 8: Auxiliary Winding Currents of the Proposed Machine

IV. Discussion

Figure 5 shows the rotor speed response of the proposed machine in which initial transient and overshoot are observed before the motor reaches the synchronous speed within 0.94 s. Load application of 20 Nm at 5 seconds caused transient and in this case, the motor goes into a shorter transient period and takes 0.4 s to reach steady-state

Figure 6, which depicts the electromagnetic torque of the proposed machine, there was an initial torque build-up with a rise of 198.66 Nm in 0.029 seconds before settling at zero. On the application of a load of 20 Nm at 5 s, a transient rise of 33.31 Nm was witnessed but settled to steady-state within 0.598 s

The main winding current of the proposed machine is presented in Figure 7. From the figure, an initial current transient rise of 126.6 A in 0.031 s was observed at start-up but settled at 6.01 A after 3 s. After the introduction of a load of 20 Nm at 5 s, a current transient rise of 12.83 A was seen but returned to steady-state after 0.305 s.

Figure 8 presents the current in the auxiliary winding of the proposed machine. At the start-up of the motor, an initial current transient of 20.99 A in 0.039 s was noticed but later settled at 5.178 A after 0.566 s.

V. Conclusion

The paper presents a comprehensive dynamic mathematical model of an interior permanent magnet synchronous motor with two independent stator windings using rotor reference frame. The simulation results of the dynamic analysis showed that the injection of leading current into the auxiliary winding contributed significantly to reduction of high inrush current drawn by the machine. Furthermore, it is obvious from the speed response characteristic that the motor attained steady state mode within a short time interval after the high starting torque, which is better than the conventional permanent magnet synchronous motor.

References

- [1]. Alger, P. L., Freiburghouse, E. H. and Chase, D. D. Double Windings for Turbine Alternators. American Institute of Electrical Engineers Transactions, (1930); 226 - 244.
- [2]. Basak, S. and Chakraborty, C. Dual Stator Winding Induction Machine: Problems, Progress and Future Scope. Institute of Electrical and Electronics Engineers Transactions on Industrial Electronics.(2015); 62 (7): 4641 - 4652.
- [3]. Munoz, A. R., Lipo, T. A. Dual Stator Winding Induction Machine Drive. Institute of Electrical and Electronics Engineers Transactions on Industry Applications.(2000);36 (5): 1369 - 1379.
- [4]. Vinodh, B. and Rao, C. M. Induction Machine Drive with Dual Stator Winding. International Journal and Magazine of Engineering, Technology, Management and Research.(2015); 2 (7): 1 - 11.
- [5]. Nisha, G. K. and Parvathi, M. S. State of Art of PMSM Speed Control using DTC and FOC Techniques. International Journal of Advanced Research in Electrical, Electronics and Instrumentation Engineering.(2016);5 (6): 4716 – 4721.
- [6]. J Obe, E. S. Steady-state Performance of a Line-start Synchronous Reluctance Motor with Capacitive Assistance. Electric Power Systems Research.(2010);80 (7): 1240 -1246.
- [7]. Ong, C. Dynamic Simulation of Electric Machinery using MATLAB/Simulink, Prentice Hall PTR, New Jersey.(1998).
- [8]. Zhao, W., Lipo, T. A. Life and Kwon, B. Dual-stator Two-phase Permanent Magnet Machines with Phase-group Concentrated-Coil Windings for Torque Enhancement. IEEE Transactions on Magnetics.(2015);53 (11): 1 - 4.
- [9]. Pillay, P. and Krishnan, R. Modelling, Simulation and Analysis of Permanent Magnet Motor Drives I. Institute of Electrical And Electronics Engineers Transactions on Industry Applications.(1989);25 (2): 265 - 273.
- [10]. Kulkarni, S. S. and Thosar, G. A. Mathematical Modeling and Simulation of Permanent magnet Synchronous Machine. International Journal of Electronics and Electrical Engineering.(2013);1(2): 66 - 71.
- [11]. Anih, L. U. and Obe, E. S. Performance Analysis of a Composite Dual-winding Reluctance Machine. Energy Conversion and Management.. (2009);50(12): 3056 - 3062.

Onah, C. O. “Modeling of an Interior Permanent Magnet Synchronous Motor with Two Independent Stator Windings using Rotor Reference Frame.” *IOSR Journal of Electrical and Electronics Engineering (IOSR-JEEE)*, 15(1), (2020): pp. 20-27.